

Controlling Bending and Twisting of Conjugated Polymers via Solitons

Xi Lin,¹ Ju Li,² and Sidney Yip^{1,*}

¹*Department of Nuclear Science and Engineering and Department of Materials Science and Engineering, Massachusetts Institute of Technology, Cambridge, Massachusetts 02139, USA*

²*Department of Materials Science and Engineering, Ohio State University, Columbus, Ohio 43210, USA*
(Received 15 June 2005; published 3 November 2005)

A strong generic coupling between self-localized solitons and conformations of a π -conjugated polymer chain is demonstrated through *ab initio* calculations and the underlying mechanisms revealed by using an extended Hubbard model. We show that significant chain bending and twisting of *trans*- and *cis*-polyacetylene result from torque imbalances among atom-centered orbitals and the steric instability at single-bond *cis*-centers, respectively. The soliton-induced conformational effects create sufficient strains to provide an intrinsic high-strain-rate actuation mechanism in optical excitation processes.

DOI: 10.1103/PhysRevLett.95.198303

PACS numbers: 82.35.Cd, 62.25.+g, 71.38.-k, 72.15.Nj

Electro or optoactive conjugated polymers are promising materials for mechanical actuation at bulk and single-molecule levels [1–3]. Such polymer chains are well known for strong electron-phonon interactions, which upon redox lead to the formation of self-localized mobile carriers known as solitons [4]. At present their functional applications are hampered by a lack of fundamental understanding and, other than certain specific molecular constructions [5–7], control of underlying actuation mechanisms. In this work, a generic coupling between solitons and the conformations of a conjugated polymer chain is revealed through *ab initio* calculations, and elucidated with insights derived from an extended Hubbard model considering electron and phonon interactions beyond nearest neighbors. We present a mechanistic analysis of two complementary conjugated polymers, *trans*- and *cis*-polyacetylene (PA). In *t*-PA we find significant in-plane chain bending due to an imbalance in second-neighbor interactions among atom-centered soliton and valence orbitals. In *c*-PA an out-of-plane chain torsion arises from third-neighbor steric interactions at the single-bond *cis*-centers. Our results, taken together with related processes occurring in PA derivatives [8,9], point to an intrinsic actuation mechanism and a central role of the soliton that has not been previously recognized.

We perform full-geometry optimizations on PA chains up to 161 units by Hartree-Fock (HF) and on shorter PA chains up to 41 units by the second-order-truncated Møller-Plesset correlation energy corrections (MP2) methods [10], with and without counterions. The HF results are found to be qualitatively similar to those obtained by MP2, both being insensitive to the choice of 3–21G or 6–31G(d) basis sets [9]. Even without the counterions, we observe strongly self-localized electronic states that induce bend and twist of the backbone, along with the more well-known changes in the C-C bond length alternation pattern. As an aside, we note that existing density functionals are known to fail to produce self-localization [9,11–13]. We first

examine the bending deformation in *t*-PA which is shown in Fig. 1. A striking feature is that chain bending occurs in *opposite* directions for the $+e$ (S^+) and $-e$ (S^-) solitons. Since positive and negative charges appear on the same side of the chain, one would expect the bending to occur in the *same* direction if the deformation were caused by simple electrostatic repulsion. To rationalize this rather counterintuitive conformational change, we adopt the Hubbard model as an extension of the conventional Su-Schrieffer-Heeger (SSH) Hamiltonian (H_{SSH}) [14]. Following standard notations, the total Hamiltonian that explicitly includes the dependence of backbone bending angles $\{\theta_n\}$ and torsion angles $\{\phi_n\}$ can be expressed as

$$\begin{aligned}
 H &= H_{SSH} + \sum_{i=0}^3 H_{0i}^{ee} + \sum_{i=2}^3 H_{0i}^{ep}, \\
 H_{00}^{ee} &= \frac{U}{2} \sum_{n,\sigma} c_{n,\sigma}^\dagger c_{n,\sigma} c_{n,\sigma}^\dagger c_{n,-\sigma}, \\
 H_{0i}^{ee} &= \sum_n V_{0i}(\theta_{n+1}, \dots, \theta_{n+i-1}, \phi_{n+2}, \dots, \phi_{n+i-1}) \\
 &\quad \times \left(-1 + \sum_{\sigma} c_{n,\sigma}^\dagger c_{n,\sigma} \right) \left(-1 + \sum_{\sigma'} c_{n+i,\sigma'}^\dagger c_{n+i,\sigma'} \right), \\
 &\quad i = 1, 2, 3 \\
 H_{02}^{ep} &= \sum_{n,\sigma} \beta(\theta_{n+1}) (c_{n+2,\sigma}^\dagger c_{n,\sigma} + c_{n,\sigma}^\dagger c_{n+2,\sigma}), \\
 H_{03}^{ep} &= \sum_{n,\sigma} \gamma(\theta_{n+1}, \theta_{n+2}, \phi_{n+2}) (c_{n+3,\sigma}^\dagger c_{n,\sigma} + c_{n,\sigma}^\dagger c_{n+3,\sigma}),
 \end{aligned} \tag{1}$$

where $c_{n,\sigma}^\dagger$, $c_{n,\sigma}$ creates and destroys a π electron of spin σ on site n , respectively. Electron-electron interactions are described by the U and V terms representing on- and off-site Coulomb repulsion, while electron-phonon interactions are expressed through the β and γ terms which involve second- and third-neighbor interactions. Extensive

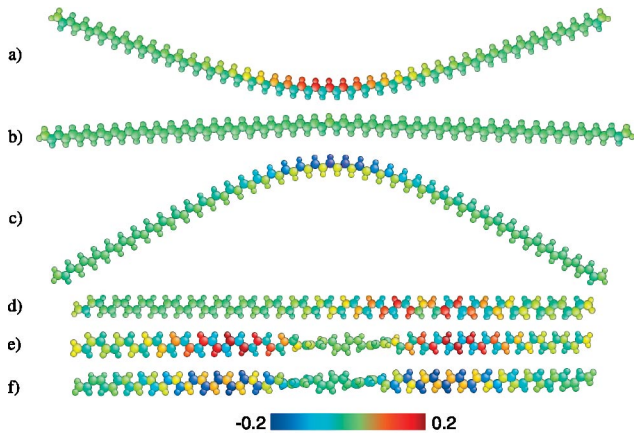


FIG. 1 (color online). Bending and torsional distortions and localized charges in *t*-PA [(a), (b), and (c)] and *c*-PA [(d), (e), and (f)]: (a) $+e$, (b) neutral, (c) $-e$ solitons, (d) a $+e$ polaron, (e) a $+2e$ bipolaron, and (f) a $-2e$ bipolaron. Mulliken charges of CH groups are color coded after subtracting off the nuclear charges.

studies of electron and phonon coupling between first neighbors exist in the literature [4,15,16]; on the other hand, there has been little work explicitly investigating the effects of more distant neighbor interactions. As we now demonstrate, these effects are responsible for the significant conformation changes seen in Fig. 1.

Because of the zigzag structure of *t*-PA, both the soliton state and the valence (π -bonding) and conduction (π -antibonding) bands respond strongly to the presence of second-neighbor hopping β terms in Eq. (1). To understand the mechanism by which these responses translate into chain deformation forces, we examine the phases of the associated soliton and valence-band wave functions. Figure 2 shows the distribution of phases along the chain (same coordinate system for all cases, with upward and downward pointing CH units labeled as even and odd sites, respectively, and the soliton positioned at the center of the chain on an even atom). As indicated by the red and blue lobes in Fig. 2(c'), the soliton wave function is localized at the even sites and has nodes at the odd sites [17]. This alternating phase between the second-neighbor sites results in repulsions when the β terms are switched on, thereby acting to bend the chain downward. For the bottom valence and top conduction states, the wave functions at the second-neighbor sites have the same phases; the forces due to the β terms are therefore attractive between both even-even and odd-odd sites. Moreover, in the absence of the electron-electron couplings indicated in Eq. (1), the forces generated by the valence states do not cause bending because the band orbitals are *bond centered* and therefore the torques are in balance between the even-even and odd-odd sites. This explains the essentially zero conformational distortion for the neutral soliton (S^0) shown in Fig. 1(b), which also would be the “conventional behavior” if the β term interactions were not considered at all. The slight

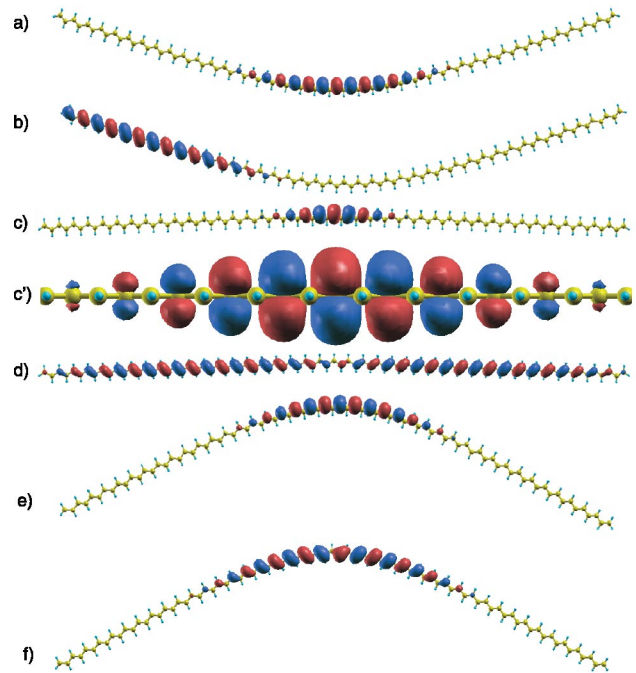


FIG. 2 (color online). Wave function contour (isosurface value $\pm 0.01 \text{ \AA}^{-3/2}$) of an 81-unit *t*-PA chain: (a) the soliton state and (b) the top valence-band state of a $+e$ soliton; (c) the soliton state, (c') a close side view of (c), and (d) the top valence-band state of a neutral soliton; (e) the soliton state and (f) the top valence-band state of a $-e$ soliton. Wave function phases (+, red and -, blue) are color coded and carbon and hydrogen denoted by golden and cyan balls, respectively. The enhanced atom-center character of the band states due to electron-electron interactions can be discerned clearly at the wave function tails.

downward bending is due to the singly occupied soliton state, which is strongly resisted by the band states.

To further emphasize the significance of the spatial nature of forces generated in response to second-neighbor coupling, we summarize our results of direct numerical solutions [under the HF approximation [15]] to the Hubbard model, where in a chain with a charged soliton, the valence and conduction states acquire atom-centered characteristics through the U and V terms in Eq. (1). Because of the fundamental band gap, the band reconstructions are mainly among themselves in response to the soliton charge [18]. For a chain with soliton S^+ , we find greater atom-centered occupancy at the *even* sites (and in-phase) relative to the odd sites for the *bottom valence* states, which is reasonable because it is energetically favorable to have more electron distributions on the positively charged (even) sites. In turn, for the *top valence* states greater atom-centered occupancy is left at the *odd* sites (but out-of-phase); see, for example, the wave function of the top valence-band state in Fig. 2(b). The entire valence band therefore acts in unison to give rise to an upward bending of the chain as seen in Fig. 1(a), with

attractive even sites due to the bottom valence states and repulsive odd sites due to the top valence states. The opposite occurs in the case of soliton S^- : greater occupancy is generated at the *odd* sites (in-phase) for the bottom valence electrons and at the *even* sites (out-of-phase) for the top valence electrons, the latter being illustrated in Fig. 2(f). Now the effect on chain conformation is to move the even sites away from each other, causing a downward bending.

Combining the effects of the soliton state and the valence band gives a mechanistic interpretation of three bending distortions shown in Fig. 1, namely, an upward bending, slight downward bending, and downward bending for the three soliton charge states with zero, single, and double occupancy. For S^+ the upward chain bending is due to the valence-band action only. For S^0 the atom-centered soliton and bond-centered valence-band responses work against each other at small bending angles, leaving a chain conformation with only a slight downward bent. For S^- the two responses act in the same direction to bend the chain downward. Before leaving this discussion we note that the slight downward bending in S^0 implies that the valence band response of S^0 is an even function of the bending angle θ , with leading terms $\sim\theta^2$ for small θ , whereas the soliton response is an odd function of θ , which therefore would dominate at small θ .

Our interpretations are corroborated by a quantitative examination of how the energies of the various electronic eigenstates change with chain conformation, shown in

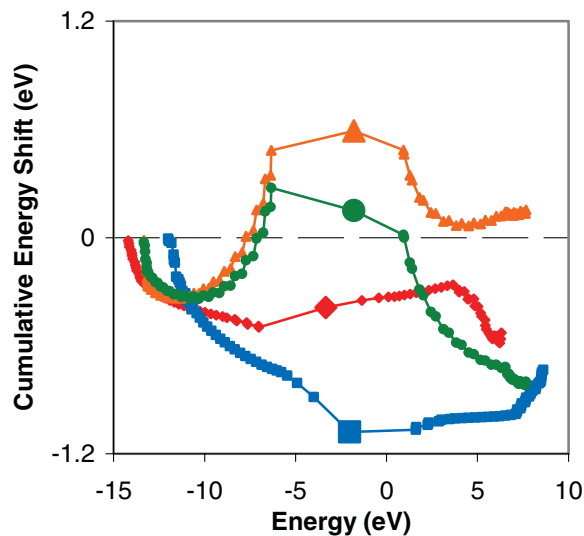


FIG. 3 (color online). Cumulative π -band energy shifts of bending conformations with respect to corresponding straight conformations: a neutral 81-unit t -PA bending upward (orange triangles) and downward (green circles), a $+e$ soliton bending upward (red diamonds), and a $-e$ soliton bending downward (blue squares). Soliton states are marked with big symbols (singly occupied in neutral, doubly occupied in $-e$, and unoccupied in $+e$ solitons).

Fig. 3. We label the discrete states according to their eigenenergies (the x axis). Against this we plot the cumulative energy shift, defined as the sum of the individual eigenenergy shifts of states lying from the bottom of the valence band up to the state in question. By energy shift we mean the difference between the energies of a state when the chain is bent and when it is straight. In the two curves labeled by red diamonds (S^+) and blue squares (S^-) we see energy shifts becoming increasingly negative as one moves up the band. Going from the top of the valence band to the soliton state, the curves show opposite behavior, an *increase* of 0.1 eV for S^+ , and a *decrease* of 0.2 eV for S^- . The implication is that the valence band and the soliton responses to the β terms oppose each other in the first instance and in the second instance they complement. Thus the detailed energetics of the system give a picture fully consistent with our foregoing interpretations.

Turning to c -PA, the *effective* second-neighbor interactions from the V_{03} and γ terms in Eq. (1) give rise to torsional distortions of the backbone. The reason that a neutral c -PA, the $+1$ phase in Fig. 4, is metastable as a planar chain has to do with having double bonds at the *cis* centers, and the fact that the -1 phase, where two closely situated double bonds repel, is energetically unfavorable. Upon the formation of a $+e$ soliton-antisoliton pair (polaron), the order parameter reaches zero (magenta triangles), indicating the presence of partial double bonds at the *cis* centers in the polaron core regions. In this case c -PA remains planar [Fig. 1(d)]. However, when the $\pm 2e$ soliton-antisoliton pair (bipolaron) is formed, the order

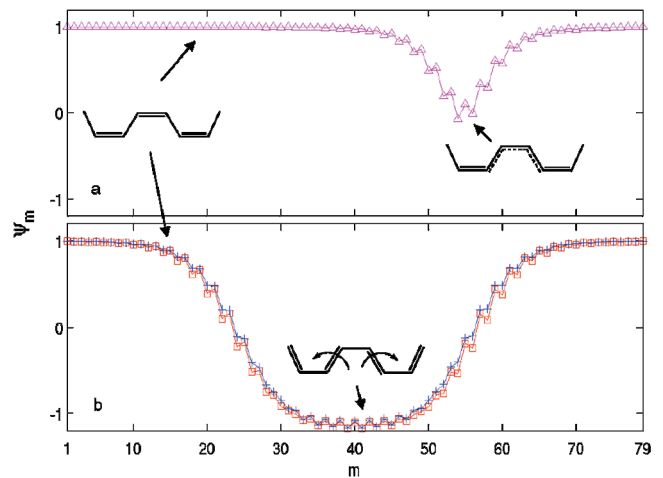


FIG. 4 (color online). Bond length order parameter profiles $\psi_m = (-1)^m(d_m - d_{\text{mean}})/d_{\text{diff}}$ showing the presence of localized soliton states in an 80-unit c -PA, where d_m is the absolute bond length, d_{mean} and d_{diff} are the average and difference bond lengths of the long and short bonds of a perfectly dimerized chain: (a) a $+e$ polaron (magenta triangles) and (b) a $+2e$ bipolaron (red squares) and a $-2e$ bipolaron (blue pluses). Boundary effects of a finite chain are eliminated by comparison to polaron/soliton-free chain.

parameter reaches the -1 phase which creates single bonds at the *cis* centers. The steric repulsion between two closely positioned double bonds thus causes the CH units to twist at the single-bond centers, these situations being depicted in Figs. 1(e) and 1(f). To complete the picture it is worthwhile to compare the present *c*-PA with a polypyrrole chain which also contains a *cis*-carbon backbone. The presence of aromatic pyrrole rings gives an opposite energetic ordering for the neutral chains, favoring the -1 phase rather than the $+1$ phase. One therefore expects to have *twisted* neutral polypyrrole chains and *planar* charged polypyrrole chains, which is what detailed calculations show [9]. The broader implication is that in *cis*-carbon backbones strong third-neighbor steric repulsions can give rise to a rich variety of conformational changes upon the creation and annihilation of polarons, especially in the case of nonparallel torsion axes, such as the bridge bonds in polypyrrole [9].

In this work we analyze two complementary prototype conjugated polymer chains to demonstrate soliton-induced conformational changes as a natural extension to the traditional soliton theory. Neutral straight *t*-PA bends upon doping due to second-neighbor interaction imbalances of the backbone, while twisting occurs in neutral planar *c*-PA due to third-neighbor torsions of the backbone. We find that the soliton-induced bending and torsion motions retain in the presence of various counterions, including F^- , ClO_4^- , PF_6^- , SO_4^{2-} , Li^+ , and Na^+ . In view of the generic nature of self-localized charged solitons we believe that the distortions in conjugated polymers are fundamental to understanding large conformational changes in polymer chains containing *trans*- and *cis*-carbon backbones. Estimates of mechanical properties indicate that end-to-end molecular strains of 10% should accompany the conformational changes calculated here. This suggests an alternative molecular actuation mechanism to the widely recognized counterion volume insertion effect occurring in bulk polymers [5]. Because soliton mobility is much greater than that of counterions, the soliton conformation coupling analyzed here could lead

to a new class of high-strain-rate actuators controlled by optical excitations [2].

The authors would like to acknowledge support by Honda R&D Co., Ltd., DARPA/ONR, AFOSR, NSF under Grants No. ITR-020541, No. DMR-0325553, and No. IMR-0414849, LLNL, and the OSU Transportation Research Endowment Program.

*To whom correspondence should be addressed.

Electronic mail: syip@mit.edu

- [1] W. Lu *et al.*, Science **297**, 983 (2002).
- [2] T. Hugel *et al.*, Science **296**, 1103 (2002).
- [3] Y. Yu, M. Nakano, and T. Ikeda, Nature (London) **425**, 145 (2003).
- [4] A. J. Heeger *et al.*, Rev. Mod. Phys. **60**, 781 (1988).
- [5] T. F. Otero, in *Handbook of Organic Conductive Molecules and Polymers*, edited by H. S. Nalwa (Wiley, New York, 1997), Vol. 4, p. 517.
- [6] J. Kim and T. M. Swager, Nature (London) **411**, 1030 (2001).
- [7] J. D. Badjic *et al.*, Science **303**, 1845 (2004).
- [8] R. MacKenzie, J. M. Ginder, and A. J. Epstein, Phys. Rev. B **44**, 2362 (1991).
- [9] X. Lin *et al.*, Int. J. Quantum Chem. **102**, 980 (2005).
- [10] M. J. Frisch *et al.*, computer program GAUSSIAN03 (Gaussian, Inc., Pittsburgh PA, 2003).
- [11] V. M. Geskin, A. Dkhissi, and J. L. Brédas, Int. J. Quantum Chem. **91**, 350 (2003).
- [12] L. Zuppiroli *et al.*, Chem. Phys. Lett. **374**, 7 (2003).
- [13] M. van Faassen *et al.*, Phys. Rev. Lett. **88**, 186401 (2002).
- [14] W. P. Su, J. R. Schrieffer, and A. J. Heeger, Phys. Rev. Lett. **42**, 1698 (1979).
- [15] K. R. Subbaswamy and M. Grabowski, Phys. Rev. B **24**, 2168 (1981).
- [16] M. J. Dewar, *The Molecular Orbital Theory of Organic Chemistry* (McGraw-Hill, New York, 1969).
- [17] W. P. Su, J. R. Schrieffer, and A. J. Heeger, Phys. Rev. B **22**, 2099 (1980).
- [18] X. Lin *et al.* (to be published).